Enhanced tumorigenesis in HTLV-1 Tax-transgenic mice deficient in interferon-gamma

Shibani Mitra-Kaushik, John Harding, Jay Hess, Robert Schreiber, and Lee Ratner

The oncoprotein Tax of human T-cell leukemia virus type I (HTLV-1) is the major mediator of viral pathogenesis in infected individuals. Expression of Tax under the regulation of the human granzyme B promoter in mice results in a lymphoproliferative disorder resembling adult T-cell leukemia/lymphoma (ATL). Tax expression is associated with the production of high levels interferon-γ (IFN-γ) in HTLV-1–infected CD4$^+$ cells and Tax-transgenic tumors. We examined the role of IFN-γ in tumorigenesis, by mating Tax-transgenic mice with a gene-specific knockout for IFN-γ. IFN-$\gamma^{-/-}$ Tax$^+$-transgenic mice show accelerated tumor onset (median, 4 versus 6 months), dissemination (median, 5 versus 7 months), and death (median, 7 versus 10 months), compared with IFN-$\gamma^{+/-}$ or IFN-$\gamma^{+/+}$ Tax$^+$ mice. Pathologic and immunophenotypic characteristics of tumors from all genotypes are indistinguishable, except for enhanced interleukin 2 receptor–β (IL-2Rβ) and suppressed intercellular adhesion molecule–1 (ICAM-1) expression on tumors from IFN-$\gamma^{-/-}$ Tax$^+$ transgenic mice. IFN-$\gamma^{-/-}$ tumors demonstrate enhanced CD31 (platelet-endothelial CAM-1 [PECAM-1]) staining compared with those from IFN-$\gamma^{+/-}$ or IFN-$\gamma^{+/+}$ Tax$^+$ mice. Angiogenesis-specific cDNA microarray analysis identified 4 mediators of angiogenic growth differentially expressed in tumors from Tax$^+$IFN-$\gamma^{-/-}$ mice compared with Tax$^+$IFN-$\gamma^{+/+}$ littermates. As confirmed by reverse transcription–polymerase chain reaction (RT-PCR), loss of IFN-γ results in down-regulation of tumor necrosis factor–α (TNF-α) and tissue inhibitor of matrix metalloproteinase-1 (TIMP-1) while up-regulating expression of vascular endothelial growth factor (VEGF) and tenascin C. These results provide insight into a possible mechanism by which IFN-γ contributes to host resistance against HTLV-induced tumors through an angiostatic effect. (Blood. 2004;104:3305-3311)

Introduction

Human T-cell leukemia virus type I (HTLV-1), which belongs to the oncoretrovirus family, is the etiologic agent of 2 different diseases: adult T-cell leukemia/lymphoma (ATL) and the neurologic disorder tropical spastic paraparesis/HTLV-1–associated myelopathy.[1-3] The 40 kDa transactivator protein Tax mediates the transition from latency to virus production by interacting with specific host proteins associated with cellular transcriptional pathways, such as nuclear factor–κB (NFκB), cyclic AMP–response element binding protein (CREB)/activating transcription factor (ATF), serum-response factor (SRF), specificity protein–1 (SP1), and early growth response–1 (EGR-1). Through interaction with cellular transcription factors, Tax potently activates transcription not only from the viral promoter but also from the enhancer elements of many cellular genes involved in host cell proliferation.[4-8] The oncogenic potential of Tax has been demonstrated in animal models, as well as in vitro transformation assays, and activation of NFκB has been implicated as a critical feature.[9] Therefore, Tax may be responsible for many of the required events necessary for HTLV-1–mediated lymphocyte immortalization and malignancy. To understand the mechanisms involved in transformation, we have used transgenic mice expressing Tax from the human granzyme B promoter in lymphoid cells resulting in tumors at peripheral sites of the body at 6 to 9 months of age.[10] These tumors consist primarily of large granular lymphocytes (LGLs), which subsequently infiltrate secondary lymphoid organs and other visceral sites. The tumors exhibit high levels of interferon-γ (IFN-γ); interleukin-15 (IL-15); interleukin-1 (IL-1); granulocyte-monocyte colony-stimulating factor (GM-CSF); and several cell adhesion molecules such as intercellular adhesion molecule–1 (ICAM-1), very late antigen–4 (VLA-4), leukocyte function–associated antigen (LFA-1), and vascular cell adhesion molecule–1 (VCAM-1).[11] Modified levels of cytokines and adhesion molecules have been linked to organ infiltration and disease development in HTLV pathogenesis.[12-14]

IFN-γ is a pleiotropic cytokine secreted by activated T cells and natural killer (NK) cells and plays a central role in innate and adaptive arms of host antiviral and antitumor immune defense.[15,16] It acts in different ways on host and tumor cells to favor tumor regression by inducing cellular antitumor immunity, inflammation, cell cycle arrest, and apoptosis and by inhibiting angiogenesis.[17] The IFN-γ signaling pathway leads to apoptosis and to the expression of immunomodulatory proteins that aid cytotoxic T lymphocyte (CTL)–mediated destruction of tumors. Thus, it is interesting to elucidate the role of IFN-γ in Tax-mediated lymphoproliferation. In this study, we characterized cellular mechanisms that are modulated by Tax to initiate and promote tumorigenesis in the presence or absence of IFN-γ. Although Tax tumors are immunogenic and are commonly infiltrated by both CD4 and CD8 T cells, the tumors are not completely rejected by the host, and progress. There is a growing realization that many responses defined as

From the Departments of Internal Medicine, Molecular Microbiology, and Pathology, Washington University School of Medicine, St Louis, MO; and the Department of Pathology and Laboratory Medicine, University of Pennsylvania, Philadelphia, PA.

Submitted January 23, 2004; accepted May 25, 2004. Prepublished online as *Blood* First Edition Paper, August 3, 2004; DOI 10.1182/blood-2004-01-0266.

Supported by Public Health Service (PHS) grants (L.R.); Dr Michael Lairmore at the Ohio State University through a program project; and Pharmacia.

Reprints: Lee Ratner, Department of Internal Medicine, Washington University School of Medicine, 660 S Euclid Ave, Box 8069, St Louis, MO 63110; e-mail: lratner@im.wustl.edu.

The publication costs of this article were defrayed in part by page charge payment. Therefore, and solely to indicate this fact, this article is hereby marked "advertisement" in accordance with 18 U.S.C. section 1734.

anti–tumor-effector mechanisms act as double-edged swords and under different conditions become either ineffective or even protumorigenic. Examples are IL-2 (also proapoptotic for activated T cells), IFN-γ (by induction of ligands for T- and NK-cell–inhibitory receptors), angiogenesis inhibition (by hypoxia-mediated induction of growth factors promoting metastasis), and macrophage free radical–mediated cytotoxicity (by inhibiting T cells). Immune selection pressure resulting in outgrowth of resistant tumor variants could also be viewed in this light. The immense plasticity of the tumor cell and the complex balance between protumor and antitumor activity of the same effector pathways determine the fate of tumor progression. Our results indicate that while IFN-γ triggers an inhibitory mechanism in early steps of tumor initiation, growth of tumors is not completely obviated, possibly owing to the recruitment of other cellular pathways. This study defines a role played by IFN-γ in angiogenesis and oncogenesis in Tax-transgenic mice and possibly HTLV-1–associated lymphoproliferative disease.

Materials and methods

Tax-transgenic mice deficient in IFN-γ

Transgenic mice expressing HTLV-1 Tax (C57/Bl6-SJL)[10] and IFN-γ–deficient (C57/Bl6) mice with targeted gene knockout[18] have been described previously. Tax-transgenic mice were mated with IFN-γ knockout mice to generate Tax-positive, IFN-γ–heterozygous ($Tax^+IFN\text{-}\gamma^{+/-}$) offspring, which were subsequently crossed to generate a colony of Tax^+ mice with a gene knockout for IFN-γ (Tax^+ $IFN\text{-}\gamma^{-/-}$). Genotypes were ascertained by means of polymerase chain reaction (PCR) on mouse-tail genomic DNA and Southern blot hybridization.[18] The level of IFN-γ secreted in each genotype was measured by means of a sandwich enzyme-linked immunosorbent assay (ELISA)–based kit (R&D Systems, Minneapolis, MN). The ELISA was performed on cultured spleen and tumor cells from 5 mice from each genotype. Mice were housed under pathogen-free conditions according to the guidelines of the Division of Comparative Medicine, Washington University School of Medicine (St Louis, MO) throughout the study. Progress of tumor development was monitored every week, and animals were killed at the end of the experiment or if tumors grew to larger than 20 mm in diameter.

Flow cytometry

Fresh tumors were harvested from mice for experiments, and single cell suspensions depleted of erythrocytes were made in RPMI-1640 containing 10% fetal calf serum. Tumor cells were stained with antibodies for fluorescence-activated cell sorter (FACS) as follows. First, 1×10^6 cells were washed with phosphate-buffered saline (PBS) and blocked with 5μg FcBlock (Becton Dickinson, San Jose, CA) in 0.1% bovine serum albumin (BSA) for 30 minutes to prevent nonspecific antibody or protein binding. Fluorescein isothiocyanate (FITC)–tagged antibodies to CD3, CD4, NK1.1, IL-2 receptor–β (IL-2Rβ), ICAM-1, major histocompatibility complex-1 (MHC-1) $H2^b$, MHC-2 $I\text{-}A/E^b$, or the isotype control (Pharmingen, San Diego, CA) were added after a wash with flow cytometry (FCM) wash buffer (0.01% BSA in PBS). After incubation at 4°C for an hour, the cells were washed thrice in FCM wash buffer and subjected to FACS analysis on a FACSCAN (Becton Dickinson). Data were analyzed by means of Cell Quest software (Becton Dickinson).

CTL assay

First, 20×10^6 splenic lymphocytes from 3 mice of each genotype were harvested and restimulated in vitro with 2×10^6 irradiated Tax-transfected dimethylbenzanthracene-induced thymoma T-cell line (EL-4) cells. After 5 days, CTL activity was assessed with the use of the targets $Tax^+IFN\text{-}\gamma^{+/+}$ or $Tax^+IFN\text{-}\gamma^{-/-}$ tumors and EL-4 cells transfected with Tax-expressing pcDNA-3.1 plasmid or EL-4 cells transfected with pcDNA-3.1 vector at different effector-target ratios: 1:2.5, 1:5, 1:10, and 1:25. CTL activity was measured with a CTL detection kit (Roche, Mannheim, Germany) according to the manufacturer's instructions. Briefly, the effectors and 2000 target cells were plated in triplicate at different effector-target ratios in 96-well dishes for 10 to 12 hours; 100 μL cell-free culture supernatant was collected in 96-well plates and 100 μL dye substrate was added to each well. The extent of lysis of the targets was proportional to the lactate dehydrogenase (LDH) released from the cells and was detected in the culture supernatants with the use of a color reaction read at 600 nm. Experiments were performed with tissues from 3 mice with triplicates for all samples. The percentage of specific lysis was calculated by the following formula: % specific lysis = (experimental release − spontaneous release)/(total release − spontaneous release) × 100.

Immunohistochemistry

Tumors were excised from mice and fixed in 10% neutral buffered formalin for 24 hours. First, 4 μm sections were made from paraffin-embedded tissues and fixed onto glass slides. The tissue sections were deparaffinized by heating at 65°C in citrate buffer (pH, 6.5) for an hour and hydrated and fixed in 2% paraformaldehyde. The slides were then washed, blocked with 1% normal goat serum, and stained with anti–platelet-endothelial CAM-1 (anti–PECAM-1) (CD31) antibody (Santa Cruz Biotechnology, Santa Cruz, CA) for an hour. The tissues were then incubated with anti–rabbit horseradish peroxidase (HRP) antibody for 30 minutes. The secondary antibody treatment was followed by 3 washes in PBS, and finally the stain was developed by means of the ABC staining system (Santa Cruz Biotechnology). Tissues were counterstained with Harris hematoxylin no. 2, fixed, and dehydrated. Slides were visualized on a Nikon Eclipse E400 microscope (Melville, NY) with a × 10 eyepiece, × 40 lens, and a 0.75 PH2 aperture, and photographed with an Optronics MagnaFine camera (Muskogee, OK). Photographs were processed with MagnaFine 2.0 software and Adobe Photoshop 6.0 (San Jose, CA). Random fields were counted to monitor brown stained areas corresponding to angiogenic sites.

SuperArray method

Total cellular RNA was isolated from fresh tumor tissues with the use of Tri-Reagent (Life Technologies, Gaithersburg, MD). The mouse angiogenesis pathway was examined with the GEArray kit (SuperArray, Bethesda, MD; catalog no. MM-009). This kit determines differential expression levels of multiple genes involved in a biologic pathway. Briefly, the total RNA from the respective samples was used as a template to generate ^{32}P γ–adenosine triphosphate (^{32}P γ-ATP) cDNA probes with the use of the GEAprimer mix as a reverse-transcriptase primer. The cDNA probes, which represent the abundance of the mRNA population, were then denatured, and hybridization was conducted in GEHybridization solution to duplicate nylon membranes spotted with gene-specific cDNA fragments. The GEArray Q Series gene array contains 96 cDNA fragments from genes associated with the angiogenesis pathway. These cDNA fragments are printed on a 3.8 × 4.8 cm nylon membrane with an advanced noncontact printing technology. Each cDNA fragment is printed in quadruplicate, to allow multiple, simultaneous, independent measurements of a given mRNA abundance. Membranes were then washed in 2 × saline sodium citrate (SSC) and 1% sodium dodecyl sulfate (SDS) twice for 20 minutes each, followed by 0.1 × SSC and 0.5% SDS twice for 20 minutes each. The membranes were then exposed to Kodak X-Omat film (Eastman Kodak, Rochester, NY) at −70°C with intensifying screens. Color images were generated by means of UMAX flatbed scanner at a resolution of more than 300 dots per inch and processed by ScanAlyze Software (Michael Eisen, Stanford University, Palo Alto, CA) to extract the data from the scanned figure. Another software, GEArray Analyzer (SuperArray software), was used to determine the relative expression level of each gene and obtain actual tabulated values and plots. Data were corrected for equal RNA loading on the basis of the corresponding β-actin mRNA levels.

Reverse transcription–polymerase chain reaction

Total cellular RNA was isolated from $Tax^+IFN\text{-}\gamma^{+/+}$ or $Tax^+IFN\text{-}\gamma^{-/-}$ cells with the use of Tri-Reagent (Life Technologies). Contaminating DNA was

removed from these RNA aliquots by means of a DNA-*free* kit (Ambion, Austin, TX). The cDNA was synthesized from 3 or 5 μg total RNA by means of Superscript II reverse transcriptase (Invitrogen, Carlsbad, CA). Gene-specific primers were used at 10 pmole per reaction: TNF-AFor, GTCTCAAAGACAACCAACTAGTC; TNF-ARev, CTCCAGCTGGAAGACTCCTCCCAG; TIMP-1For, GGCATCCTCTTGTTGCTATCACTG; TIMP-1Rev, GTCATCTTGATCTCATAACGCTGG; VEGF-For, GATGAAGCCCTGGAGTGC; VEGF-Rev, TCCCAGAAACAACCCTAA; TenC-For, GTTTGGAGACCGCAGAGAAGAA; TenC-Rev, TGTCCCCATATCTGCCCATCA; S15-For, TTCCGCAAGTTCACCTACC; S15-Rev, CGGGCCGGCCATGCTTTACG. PCR was performed by means of Biomix Red *Taq* polymerase (Bioline, Randolph, MA). PCR products were resolved on a 1% agarose gel stained with ethidium bromide and analyzed by means of Eagle Eye (Stratagene, La Jolla, CA) and ImageQuant Software (Amersham Biosciences, Piscataway, NJ). Fold changes were calculated relative to S15 rRNA expression levels. Three independent reverse transcription PCR (RT-PCR) assays with 2 tumors from each genotype were performed for each primer set.

Tumor transplants

C57/Bl6.SJL (H-2^b) mice were purchased from Taconic (Germantown, NY). Before the challenge injection, the major histocompatibility complex (MHC)–matched (H-2^b) Tax tumor–derived SC cells[11] were harvested at log-phase in tissue culture. Live cells were counted in a hemocytometer by trypan blue exclusion. First, 5×10^6 cells were mixed with 250 μL ice-cold Matrigel (Becton Dickinson) and injected via a subcutaneous route on the back of the animals. The antibody-treated animals received 100 μg either H22 (hamster IFN-γ–neutralizing antibody)[19] or hamster anti-glutathione S-transferase (PIP), an isotype-matched control antibody preparation, on days −2, 14, and 28. The growth of each tumor, measured by the diameter of the solid tumor, the time of the appearance, and the rate of growth was measured with the use of vernier calipers in each set of animals containing 5 animals each.

Results

Early tumor onset and enhanced tumor progression lead to decreased survival in Tax-transgenic mice deficient in IFN-γ

We have generated Tax-transgenic mice with a gene-specific knockout for IFN-γ by mating the Tax^+ mice with IFN-γ knockout mice. We determined the onset of tumors, rate of dissemination of primary tumors, and finally, survival of mice in $Tax^+IFN\text{-}\gamma^{+/+}$ (n = 35), $Tax^+IFN\text{-}\gamma^{+/-}$ (n = 30), $Tax^+IFN\text{-}\gamma^{-/-}$ (n = 38), $Tax^-IFN\text{-}\gamma^{+/+}$ (n = 10), $Tax^+IFN\text{-}\gamma^{+/-}$ (n = 12), and $Tax^-IFN\text{-}\gamma^{-/-}$ (n = 20) mice. The $Tax^-IFN\text{-}\gamma^{-/-}$ mice have previously been shown to develop spontaneous adenocarcinomas and sarcomas at 1.5 to 2 years of age.[18] We found that the LGL tumors in $Tax^+IFN\text{-}\gamma^{-/-}$ mice develop at an earlier time point (4 months, median) as compared with $Tax^+IFN\text{-}\gamma^{+/+}$ $Tax^+IFN\text{-}\gamma^{+/-}$ mice (7 months median) (Figure 1A). The levels of IFN-γ were measured in tissues from each group with an IFN-γ ELISA assay, and $Tax^+IFN\text{-}\gamma^{+/+}$ and $Tax^+IFN\text{-}\gamma^{+/-}$ mice show equivalent expression of IFN-γ ("Materials and methods"; data not shown). The knockout mice had no detectable IFN-γ. $Tax^+IFN\text{-}\gamma^{-/-}$ mice also develop multiple tumors faster (Figure 1B) and succumb more rapidly owing to increased tumor burden than $Tax^+IFN\text{-}\gamma^{+/+}$ and $Tax^+IFN\text{-}\gamma^{+/-}$ mice (Figure 1C).

Pathologic and immunologic characterization of LGL tumors in $Tax^+IFN\text{-}\gamma^{-/-}$ mice as compared with $Tax^+IFN\text{-}\gamma^{+/+}$

The histologic stains of tumor tissues to evaluate morphologic details with each genotype reveal that morphologically the tumors under comparison are similar in all aspects. They are composed of LGL cells admixed with polymorphonuclear leukocytes. Fresh tumor cells from each genotype were analyzed by FACS staining to compare the cell surface phenotype of the tumors in $Tax^+IFN\text{-}\gamma^{+/+}$ and $Tax^+IFN\text{-}\gamma^{-/-}$ mice. The immunophenotypes of tumors from the $Tax^+IFN\text{-}\gamma^{+/+}$ and $Tax^+IFN\text{-}\gamma^{-/-}$ mice are quite similar, with expression of FcγRII/III but not CD3, CD4, or CD8. However, a few differences were noted (Figure 2A). The IFN-γ knockout Tax tumors display lower amounts of cell surface expression of ICAM-1, an adhesion molecule induced by IFN-γ, as compared with the $Tax^+IFN\text{-}\gamma^{+/+}$ tumors. In addition, $Tax^+IFN\text{-}\gamma^{-/-}$ tumors exhibited 2-fold higher expression of IL-2Rβ than the $Tax^+IFN\text{-}\gamma^{+/+}$ tumors.

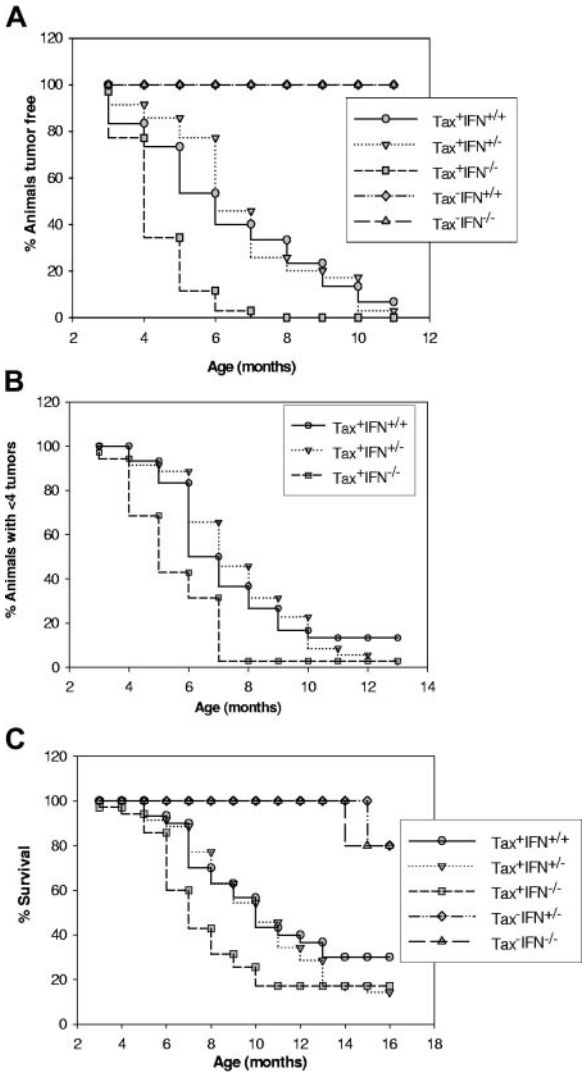

Figure 1. Analysis of tumor onset, tumor progression, and survival in wild-type (WT) and IFN-γ knockout mice. (A) Phenotype of $Tax^+IFN\text{-}\gamma^{-/-}$ mice as measured by the onset of a visible tumor mass. Mice were genotyped by means of the PCR assay described in "Materials and methods," and 38 Tax^+ mice and 20 Tax^- mice from each genotype were followed for the appearance of visible tumors at peripheral sites. The statistical significance of the observations was calculated by means of a paired *t* test in Sigma plot 2001. $Tax^+IFN\text{-}\gamma^{+/+}$ versus $Tax^+IFN\text{-}\gamma^{+/-}$ ($P \leq .21$), and $Tax^+IFN\text{-}\gamma^{+/+}$ versus $Tax^+IFN\text{-}\gamma^{-/-}$ ($P \leq .003$). (B) Progress of tumorigenesis in $Tax^+IFN\text{-}\gamma$ knockout mice as compared with Tax-transgenic mice. Animals were scored for appearance of multiple tumors (more than 4 visible tumors), and the statistical significance for the experiments was determined. $Tax^+IFN\text{-}\gamma^{+/+}$ versus $Tax^+IFN\text{-}\gamma^{+/-}$ ($P \leq .69$) and $Tax^+IFN\text{-}\gamma^{+/+}$ versus $Tax^+IFN\text{-}\gamma^{-/-}$ ($P \leq .005$). (C) Decreased survival of $Tax^+IFN\text{-}\gamma$ knockout mice. $Tax^+IFN\text{-}\gamma^{+/+}$ versus $Tax^+IFN\text{-}\gamma^{+/-}$ ($P \leq .05$) and $Tax^+IFN\text{-}\gamma^{+/+}$ versus $Tax^+IFN\text{-}\gamma^{-/-}$ ($P \leq .003$).

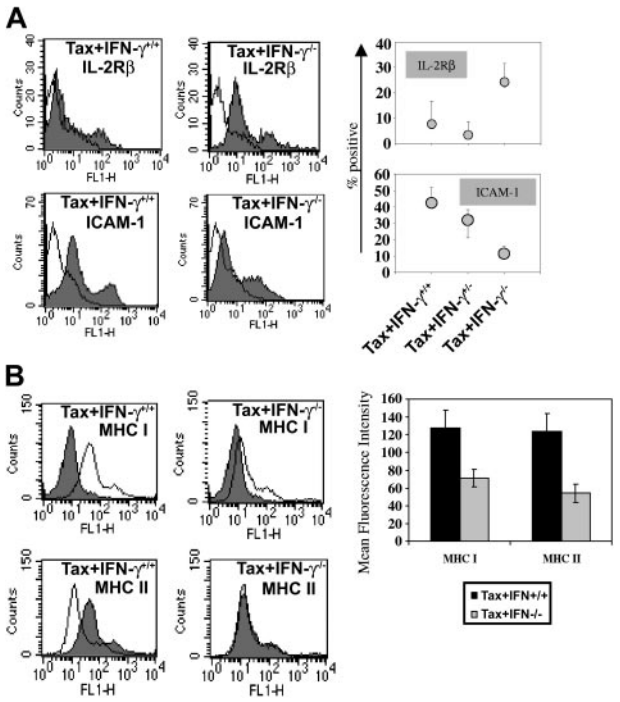

Figure 2. Adhesion molecules expressed on WT and IFN-γ knockout tumors. Fresh tumor cell suspensions from 4 tumor specimens from each genotype were stained with FITC-conjugated antibodies at a concentration of 1 μg/10^6 cells and subjected to FACS analysis. (A) FACS scans of IL-2Rβ– and ICAM-1–expressing tumor cells corresponding to one representative tumor and quantitative analysis of the percentage of positive cells in the population from 4 tumor specimens of each genotype are depicted. (B) Representative FACS histograms are shown, and quantitative mean fluorescence intensity comparisons of MHC I and MHC II stains on tumor cells are shown. There were 25 000 tumor cells counted from each tumor, and 4 tumors were analyzed for each genotype. The first peak in all 4 panels indicates isotype control. The second peak corresponds to specific staining for IL-2Rβ, ICAM-1, MHC-I, or MHC-II. Error bars represent SEM.

The IFN-γ–deficient Tax tumors show decreased levels of surface MHC I and II (Figure 2B) compared with $Tax^+IFN\text{-}\gamma^{+/+}$ and $Tax^+IFN\text{-}\gamma^{+/-}$ tumors. We expected that this decrease might reflect on the numbers of infiltrating T cells and on the ability of these cytotoxic cells to eliminate Tax-expressing tumors. However, immunostaining for CD4 and CD8 T cells in tumor tissues at early or late stages of tumor development showed no significant differences in levels of tumor-infiltrating lymphocytes (data not shown) or the total numbers of Tax-specific CTLs. The ability of the splenic T-cell population to kill Tax-expressing targets was also not affected in Tax mice deficient in IFN-γ (Figure 3). Under normal circumstances IFN-γ potentiates antitumor immune responses by mobilizing tumor-specific CTLs, NK cells, and proinflammatory cytokines and chemokines. To investigate whether the lack of differences in tumor-infiltrating lymphocytes was a result of resistance to IFN-γ of Tax-transgenic tumors, signal transducer and activator of transcription–1 (STAT-1) gel shift assays were performed with nuclear extracts from IFN-γ–treated Tax^+ tumor cells and compared with untreated cells. However, no difference of STAT-1 nuclear localization was seen (data not shown), indicating that the IFN-γR and downstream signaling was intact. Also there are no discernible differences in the levels of Tax protein in tumors from $IFN\text{-}\gamma^+$ and IFN-γ knockout mice; thus, early onset and enhanced tumorigenesis are not due to higher expression of Tax in $IFN\text{-}\gamma^{-/-}$ mice.

Effects on angiogenesis and apoptosis of LGL tumors in $Tax^+IFN\text{-}\gamma^{-/-}$ mice as compared with $Tax^+IFN\text{-}\gamma^{+/+}$ mice

IFN-γ has been implicated in the regulation of angiogenesis during tumor development.[17] Therefore, tissue sections of Tax^+ tumors were analyzed by immunohistochemical staining with a murine CD31 (PECAM-1) antibody to estimate differences in tumor vascularity (Figure 4A). Tumors deficient in IFN-γ displayed 1.6- to 1.9-fold higher rate of angiogenesis, using mean vessel density as a measure of neovascularization (Figure 4B). Since IFN-γ also induces apoptosis in several human tumors,[20,21] the number of apoptotic cells in tumors was determined from similar tissue sections by means of a transferase-mediated deoxyuridine triphosphate nick-end labeling (TUNEL) assay. There were no disernible differences in the numbers of apoptotic cells in tumors from $Tax^+IFN\text{-}\gamma^{-/-}$ mice compared with $Tax^+IFN\text{-}\gamma^{+/+}$ mice (data not shown).

Effects of IFN-γ deficiency on angiogenic gene expression in LGL tax tumors

The transcriptional profiles of $Tax^+IFN\text{-}\gamma^{+/+}$ and $Tax^+IFN\text{-}\gamma^{-/-}$ tumors were examined by cDNA microarray hybridization analysis and confirmed by RT-PCR assays (Figure 5). This study examined transcripts induced or repressed at least 2-fold from an array of 96

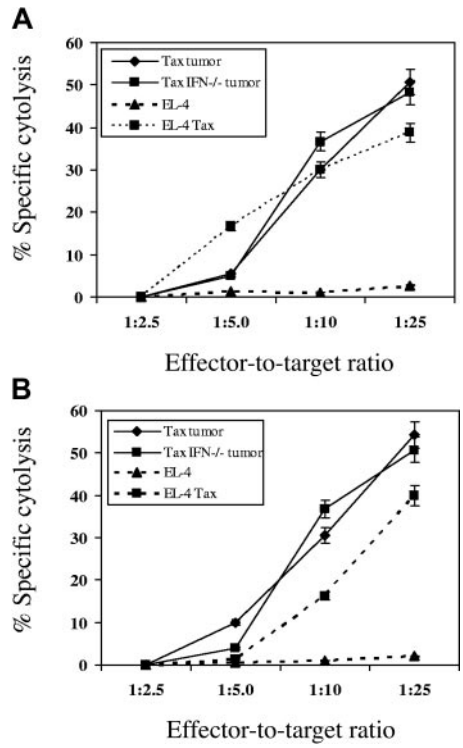

Figure 3. CTL response not affected in IFN-γ knockout tumors. (A) CTL lysis of $Tax^+IFN\text{-}\gamma^{+/+}$ and $Tax^+IFN\text{-}\gamma^{-/-}$ tumors by in vitro–stimulated Tax^+ splenocytes. In vitro–restimulated splenic lymphocytes from 3 mice were used to measure the ability of Tax-specific CTLs to lyse specific targets from $IFN\text{-}\gamma^+$ and knockout Tax tumor cells at different target-effector ratios, in triplicate in a 24-hour LDH release CTL assay, as described in "Materials and methods." MHC-matched EL-4 and Tax-transfected EL-4 targets were used as controls in a similar CTL lysis assay. Standard error of the mean (SEM) is represented as error bars. (B) CTL lysis of $Tax^+IFN\text{-}\gamma^{+/+}$ and $Tax^+IFN\text{-}\gamma^{-/-}$ tumors by in vitro–stimulated splenocytes from IFN-γ[εν] deficient Tax mice. Graph represents the cytolytic T-cell profile in $Tax^+IFN\text{-}\gamma^{-/-}$ (spleen T) cells upon in vitro stimulation with Tax expressing EL-4 cells. Vector DNA–transfected EL-4 cells were used as targets to measure background lysis. Error bars correspond to SEM of triplicate samples from 3 mice.

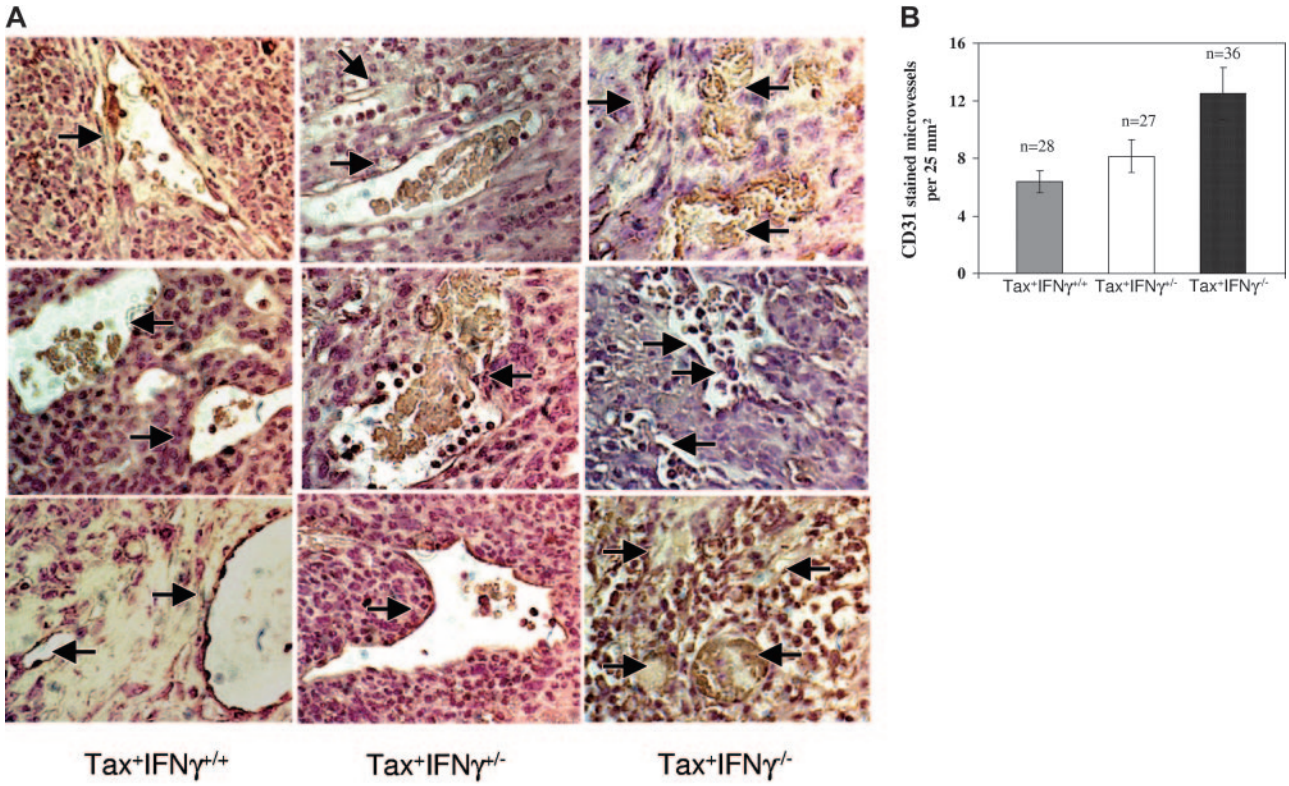

Figure 4. Angiogenesis in WT and IFN-γ knockout tumors. (A) CD31 (PECAM-1) staining for qualitative analysis of microvessel density Paraffin-embedded tissue sections were subjected to deparaffinization, rehydration, and antigen unmasking as described in "Materials and methods." At least 4 tumor specimens were stained for each genotype as follows: each slide was incubated with 5μg/mL CD31 antibody diluted in 1% normal goat serum for 1 hour at room temperature, and the bound antibody was stained by means of the ABC immunohistochemistry kit with the use of streptavidin-HRP. The slides were counterstained in Harris hematoxylin and mounted. (B) Quantitation of angiogenesis in WT and IFN-γ knockout tumors. The tissues were observed under a bright-field microscope for quantitative evaluation of positively stained blood vessels or angiogenic areas at 200 × magnification. The numbers of fields quantitated are denoted as n values. The statistical significance for analysis was established with a paired *t* test as follows: $Tax^+IFN\text{-}\gamma^{+/+}$ versus $Tax^+IFN\text{-}\gamma^{+/-}$ ($P \leq .11$); $Tax^+IFN\text{-}\gamma^{+/-}$ versus $Tax^+IFN\text{-}\gamma^{-/-}$ ($P \leq .03$); and $Tax^+IFN\text{-}\gamma^{+/+}$ versus $Tax^+IFN\text{-}\gamma^{-/-}$ ($P \leq .002$). Error bars correspond to SEM.

genes associated with angiogenesis. The GEArray is a commercially available membrane that has 4 closely placed spots for each of the 96 genes on the membrane. The microarray hybridization was performed on 2 tumors each and repeated twice to rule out false positives or negatives. The gene spots were evaluated by means of ScanAlyze software, which provides fold induction or repression in a statistically significant format after comparison of all the 4 spots for each gene analyzed. Tumor necrosis factor–α (TNF-α) and tissue inhibitor of matrix metalloproteinase-1 (TIMP-1), which inhibit the initiation and maturation of neovasculature, were down-regulated 15- and 6-fold, respectively. On the other hand, increased vascular endothelial growth factor (VEGF) (10-fold) and tenascin C (3-fold) may contribute to enhanced angiogenic growth in $Tax^+IFN\text{-}\gamma^{-/-}$ tumors compared with $Tax^+IFN\text{-}\gamma^{+/+}$ tumors.

Enhanced growth of transplanted Tax tumors in IFN-γ–deficient mice and IFN-γ–depleted mice

SC, a Tax tumor–derived cell line, when administered subcutaneously with Matrigel, a basement-membrane–derived collagen matrix, results in solid subcutaneous tumors in wild-type mice. To confirm the results obtained in transgenic mice, we injected SC cells into wild-type C57/Bl6 SJL mice and IFN-γ knockout mice. All 5 animals in the IFN-γ–deficient group were tumor positive by day 8 following tumor transplantation while tumor growth was observed in IFN-γ wild-type mice only by day 22 after transplantation. Similar results were obtained in IFN-γ wild-type animals when IFN-γ is neutralized with an H22 antibody, as compared with the control antibody group. Figure 6 shows the percentage of tumor-positive animals in each of the 4 groups of animals.

Discussion

We have demonstrated that IFN-γ contributes to anti–tumor-effector functions that may control the initiation, growth, or spread of Tax-transgenic tumors in mice. However, since mice deficient in IFN-γ also develop tumors, it appears that Tax-induced tumor initiation involves other components in cellular transformation pathways and immune responses in addition to IFN-γ. Two earlier studies have elucidated a role for IFN-γ in tumor immune surveillance.[22,23] Although originally defined as an agent with direct antiviral activity, IFN-γ regulates several aspects of the immune response, including antigen presentation by up-regulation of major histocompatability complex class I and II molecules,[24] leukocyte-endothelium interactions,[24,25] cell proliferation,[26] sensitivity to apoptosis,[27,28] stimulation of the bactericidal activity of phagocytes,[24] and down-regulation of angiogenesis.[29,30] The IFN-γ gene is transcriptionally activated by the Tax protein[31] in HTLV-infected CD4 T cells and in Tax-transgenic tumor cells.[11,32] Tax-mediated IFN-γ production results from activation of NFκB, and high levels of IFN-γ in infected cells and transgenic cells lead to a constitutively activated Janus kinase–STAT (JAK-STAT) pathway, and increased levels of ICAM-1 expression.

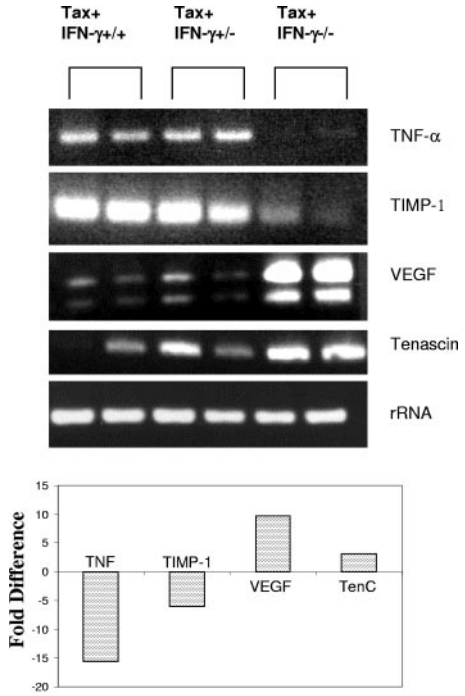

Figure 5. RT-PCR confirmation of differential gene expression. Two tumor samples from each genotype were used to extract total RNA. First, 2 to 5 μg total RNA from tumor tissues was reverse transcribed, and one-twentieth of each reaction was subjected to PCR amplification with the use of gene-specific primers as described in "Materials and methods." RT-PCR assays were performed under linear amplification conditions. Then, 20 μL each reaction was visualized on a 1% agarose gel. S15 rRNA expression served as a control. Representative results from 1 of 3 independent experiments are shown. Fold difference of RNA expression was calculated by densitometry scanning of the agarose gels, and values from one representative experiment are shown here.

The observations on the IFN-γ knockout mice indicate that although the proproliferative and proinflammatory roles of IFN-γ are not ruled out, IFN-γ may play an active role in the immune resistance to tumor development in this model system. This might explain why mice lacking IFN-γ show earlier incidence of tumors. While the tumors developing in the IFN-γ–deficient background are pathologically similar to those in the $Tax^+IFN\text{-}\gamma^{+/+}$ mice, there are differences in the expression of cell surface molecules such as IL-2Rβ, which is a receptor subunit, used by both IL-2 and IL-15. Tax tumor cells express high levels of IL-15, but not IL-2. However, there were no significant differences in proliferation rates of these tumors in vitro, but it is conceivable that IL-15 is important during or shortly after tumor initiation. An adhesion molecule affected by IFN-γ deficiency is ICAM-1, which may be responsible for the migration of tumor cells and host cells necessary for tumor development.[33] There is a decreased expression of cell surface MHC class I and II molecules on $Tax^+IFN\text{-}\gamma^{-/-}$ tumors compared with $Tax^+IFN\text{-}\gamma^{+/+}$ tumors, but this alteration does not correlate with the ability of the host to mount an efficient CTL response to these tumors (Figure 3). We believe that the decreased levels of MHC on the surface of cells is merely a reflection of the lack of IFN-γ, but does not correlate with the ability of the T cells in spleens from either genotype to recognize and kill tumor cells or Tax protein–expressing target cells. The tumors from $Tax^+IFN\text{-}\gamma^{-/-}$ treated with IFN-γ show similar levels of STAT-1 nuclear mobilization as compared with $Tax^+IFN\text{-}\gamma^{+/+}$ tumors, ruling out the lack of responsiveness to IFN-γ.[34] There also does not appear to be any discernible change in the total numbers of tumor-infiltrating CD4 and CD8 lymphocytes. Although no differences were observed in numbers of apoptotic cells within tissues late in tumor development, significant differences might be responsible for the early onset and visceral spread in the absence of IFN-γ. Thus, IFN-γ is not the only factor that regulates tumor development and growth in our mice.

It is well known that a growing tumor requires new blood vessels.[35,36] Qin et al[37] showed that inhibition of angiogenesis by $CD4^+$ T-cell–derived IFN-γ is an effective way to reduce tumor burden, allowing other, direct-killing mechanisms to eliminate residual tumor cells. Inhibition of tumor angiogenesis mediated by infiltrating CD4 T cells is dependent on the responsiveness of the tumor cells to IFN-γ.[34,38] In other tumor models, adoptively transferred tumor-specific CD8 T-cells from IFN-γ–deficient hosts are unable to mediate angiostasis as compared with those from IFN-γ–competent mice.[37] In addition, Hayakawa et al[39] demonstrated that α-galactosyl ceramide, which activates NK and NKT cells, inhibited the early stage of subcutaneous tumor growth and tumor-induced angiogenesis. These inhibitory effects were mediated by IFN-γ produced by activated NK and NKT cells.

In the current model, tumor rejection by $CD8^+$ T-cell effectors may critically depend on their ability to produce IFN-γ to inhibit tumor angiogenesis, and further studies will determine the mechanism and cell populations in this transformation event. A significant increase in the number of microvessels was evident in IFN-γ–deficient Tax tumors compared with $Tax^+IFN\text{-}\gamma^{+/+}$ tumors. Gene expression analysis indicates that proangiogenic VEGF and tenascin C are overexpressed in IFN-γ–deficient Tax tumors. There is also a significant repression of 2 angiostatic genes, *TNF-α* and *TIMP-1*. Angiogenesis is critical for tumor progression, outgrowth, and metastatic spread of tumors.[36,40] Tumor-induced angiogenesis is up- or down-regulated by proangiogenic and antiangiogenic factors produced by tumor cells and the host microenvironment.[41] IFN-γ has been implicated in the regulation of angiogenesis during tumor development.[29,42,43] We propose that IFN-γ–mediated antiangiogenesis prevents rapid tumor burden, allowing other, perhaps direct, killing mechanisms to eliminate newly developed tumor cells and preventing metastasis. We observed significant numbers of CD4 and CD8 T-cell infiltrates in the tumors growing in both the presence and the absence of IFN-γ. Perhaps, in the IFN-γ–deficient mice, T cells arrive at the tumor site too late and are confronted with a vascularized tumor, and the initial mechanism for tumor rejection is not effective. Our results suggest that the

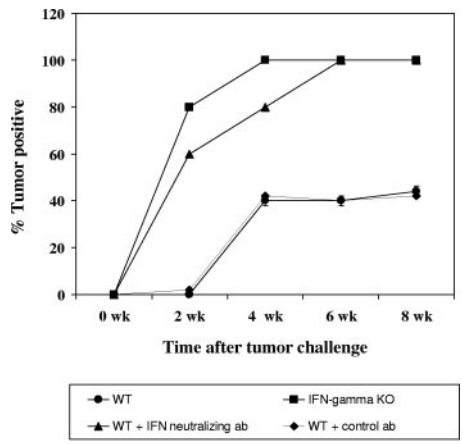

Figure 6. Tax-tumor transplantation in IFN-γ knockout mice and in mice depleted of IFN-γ. Four groups, each consisting of 5 mice, were established for this experiment as described in "Materials and methods." First, 5×10^6 SC cells were injected subcutaneously in Matrigel. Growth of tumors was observed in all animals, and the percentages of tumor-positive animals are depicted.

IFN-γ–dependent antiangiogenic effect may be one mechanism for the antitumor defense against HTLV-mediated oncogensesis.

Our results suggest that the IFN-γ–mediated inhibition of tumor angiogenesis is critically involved in the mechanisms of antitumor effects evoked by IFN-γ on Tax tumors. On the basis of the observations made in the Tax-transgenic mouse model, it will be possible to apply meaningful effort to understanding this slow but effective retrovirus in terms of its pathogenesis and immune evasion in infected hosts. The results described here provide important insights into understanding some of the difficult questions related not only to HTLV-associated leukemia and lymphoma, but also to neoplasias caused by other human pathogens (eg, Epstein-Barr virus [EBV], human herpes virus 8 [HHV8], human papillomavirus [HPV], hepatitis B virus [HBV]) that cause distinct diseases but use similar cellular pathways and mechanisms for their tumorigenesis.

Acknowledgments

We acknowledge Dr Herbert Virgin at Washington University for the gift of IFN-γ knockout mice. We thank Dr Lee Silverman at Ohio State University for review of pathologic material. Dr Yuqun Luo at Ohio State University is acknowledged for reading and critical evaluation of the manuscript.

References

1. Bangham CR. HTLV-1 infections. J Clin Pathol. 2000;53:581-586.
2. Blattner WA. Human retroviruses: their role in cancer. Proc Assoc Am Physicians. 1999;111: 563-572.
3. Uchiyama T. Human T cell leukemia virus type I (HTLV-I) and human diseases. Annu Rev Immunol. 1997;15:15-37.
4. Xiao G, Cvijic ME, Fong A, et al. Retroviral oncoprotein Tax induces processing of NF-kappaB2/p100 in T cells: evidence for the involvement of IKKalpha. EMBO J. 2001;20:6805-6815.
5. Yoshida M. Multiple viral strategies of HTLV-1 for dysregulation of cell growth control. Annu Rev Immunol. 2001;19:475-496.
6. Pise-Masison CA, Mahieux R, Radonovich M, Jiang H, Brady JN. Human T-lymphotropic virus type I Tax protein utilizes distinct pathways for p53 inhibition that are cell type-dependent. J Biol Chem. 2001;276:200-205.
7. Pise-Masison CA, Mahieux R, Radonovich M, et al. Insights into the molecular mechanism of p53 inhibition by HTLV type 1 Tax. AIDS Res Hum Retroviruses. 2000;16:1669-1675.
8. Giebler HA, Loring JE, van Orden K, et al. Anchoring of CREB binding protein to the human T-cell leukemia virus type 1 promoter: a molecular mechanism of Tax transactivation. Mol Cell Biol. 1997;17:5156-5164.
9. Sun SC, Elwood J, Beraud C, Greene WC. Human T-cell leukemia virus type I Tax activation of NF-kappa B/Rel involves phosphorylation and degradation of I kappa B alpha and RelA (p65)-mediated induction of the c-rel gene. Mol Cell Biol. 1994;14:7377-7384.
10. Grossman WJ, Kimata JT, Wong FH, Zutter M, Ley TJ, Ratner L. Development of leukemia in mice transgenic for the tax gene of human T-cell leukemia virus type I. Proc Natl Acad Sci U S A. 1995;92:1057-1061.
11. Grossman WJ, Ratner L. Cytokine expression and tumorigenicity of large granular lymphocytic leukemia cells from mice transgenic for the tax gene of human T-cell leukemia virus type I. Blood. 1997;90:783-794.
12. Alexandroff AB, McIntyre CA, Porter JC, Zeuthen J, Vile RG, Taub DD. Sticky and smelly issues: lessons on tumour cell and leucocyte trafficking, gene and immunotherapy of cancer. Br J Cancer. 1998;77:1806-1811.
13. Kodaka T, Uchiyama T, Umadome H, Uchino H. Expression of cytokine mRNA in leukemic cells from adult T cell leukemia patients. Jpn J Cancer Res. 1989;80:531-536.
14. Umehara F, Izumo S, Ronquillo AT, Matsumuro K, Sato E, Osame M. Cytokine expression in the spinal cord lesions in HTLV-I-associated myelopathy. J Neuropathol Exp Neurol. 1994;53:72-77.
15. Ichinose K, Nakamura T, Nishiura Y, et al. Characterization of adherent T cells to human endothelial cells in patients with HTLV-I-associated myelopathy. J Neurol Sci. 1994;122:204-209.
16. Ikeda H, Old LJ, Schreiber RD. The roles of IFN gamma in protection against tumor development and cancer immunoediting. Cytokine Growth Factor Rev. 2002;13:95-109.
17. Street SE, Trapani JA, MacGregor D, Smyth MJ. Suppression of lymphoma and epithelial malignancies effected by interferon gamma. J Exp Med. 2002;196:129-134.
18. Dalton DK, Pitts-Meek S, Keshav S, Figari IS, Bradley A, Stewart TA. Multiple defects of immune cell function in mice with disrupted interferon-gamma genes. Science. 1993;259:1739-1742.
19. Schreiber RD, Hicks LJ, Celada A, Buchmeier NA, Gray PW. Monoclonal antibodies to murine gamma-interferon which differentially modulate macrophage activation and antiviral activity. J Immunol. 1985;134:1609-1618.
20. Ahn EY, Pan G, Vickers SM, McDonald JM. IFN-gammaupregulates apoptosis-related molecules and enhances Fas-mediated apoptosis in human cholangiocarcinoma. Int J Cancer. 2002;100:445-451.
21. Andrews HN, Mullan PB, McWilliams S, et al. BRCA1 regulates the interferon gamma-mediated apoptotic response. J Biol Chem. 2002;277: 26225-26232.
22. Kaplan DH, Shankaran V, Dighe AS, et al. Demonstration of an interferon gamma-dependent tumor surveillance system in immunocompetent mice. Proc Natl Acad Sci U S A. 1998;95:7556-7561.
23. Dighe AS, Richards E, Old LJ, Schreiber RD. Enhanced in vivo growth and resistance to rejection of tumor cells expressing dominant negative IFN gamma receptors. Immunity. 1994;1:447-456.
24. Boehm U, Klamp T, Groot M, Howard JC. Cellular responses to interferon-gamma. Annu Rev Immunol. 1997;15:749-795.
25. Billiau A, Heremans H, Vermeire K, Matthys P. Immunomodulatory properties of interferon-gamma: an update. Ann N Y Acad Sci. 1998;856: 22-32.
26. Hawley RG, Berger LC. Growth control mechanisms in multiple myeloma. Leuk Lymphoma. 1998;29:465-475.
27. Dai C, Krantz SB. Interferon gamma induces upregulation and activation of caspases 1, 3, and 8 to produce apoptosis in human erythroid progenitor cells. Blood. 1999;93:3309-3316.
28. Tamura T, Ishihara M, Lamphier MS, et al. An IRF-1-dependent pathway of DNA damage-induced apoptosis in mitogen-activated T lymphocytes. Nature. 1995;376:596-599.
29. Coughlin CM, Salhany KE, Gee MS, et al. Tumor cell responses to IFNgamma affect tumorigenicity and response to IL-12 therapy and antiangiogenesis. Immunity. 1998;9:25-34.
30. Yao L, Sgadari C, Furuke K, Bloom ET, Teruya-Feldstein J, Tosato G. Contribution of natural killer cells to inhibition of angiogenesis by interleukin-12. Blood. 1999;93:1612-1621.
31. Brown DA, Nelson FB, Reinherz EL, Diamond DJ. The human interferon-gamma gene contains an inducible promoter that can be transactivated by tax I and II. Eur J Immunol. 1991;21:1879-1885.
32. Kubota R, Kawanishi T, Matsubara H, Manns A, Jacobson S. Demonstration of human T lymphotropic virus type I (HTLV-I) tax-specific CD8+ lymphocytes directly in peripheral blood of HTLV-I-associated myelopathy/tropical spastic paraparesis patients by intracellular cytokine detection. J Immunol. 1998;161:482-488.
33. Owen SM, Rudolph DL, Dezzutti CS, et al. Transcriptional activation of the intercellular adhesion molecule 1 (CD54) gene by human T lymphotropic virus types I and II Tax is mediated through a palindromic response element. AIDS Res Hum Retroviruses. 1997;13:1429-1437.
34. Beatty G, Paterson Y. IFN-gamma-dependent inhibition of tumor angiogenesis by tumor-infiltrating CD4+ T cells requires tumor responsiveness to IFN-gamma. J Immunol. 2001;166:2276-2282.
35. Folkman J. Tumor angiogenesis: therapeutic implications. N Engl J Med. 1971;285:1182-1186.
36. Folkman J. Angiogenesis in cancer, vascular, rheumatoid and other disease. Nat Med. 1995;1: 27-31.
37. Qin Z, Schwartzkopff J, Pradera F, et al. A critical requirement of interferon gamma-mediated angiostasis for tumor rejection by CD8+ T cells. Cancer Res. 2003;63:4095-4100.
38. Beatty GL, Paterson Y. Regulation of tumor growth by IFN-gamma in cancer immunotherapy. Immunol Res. 2001;24:201-210.
39. Hayakawa Y, Takeda K, Yagita H, et al. IFN-gamma-mediated inhibition of tumor angiogenesis by natural killer T-cell ligand, alpha-galactosylceramide. Blood. 2002;100:1728-1733.
40. Zetter BR. Angiogenesis and tumor metastasis. Annu Rev Med. 1998;49:407-424.
41. Hanahan D, Folkman J. Patterns and emerging mechanisms of the angiogenic switch during tumorigenesis. Cell. 1996;86:353-364.
42. Qin Z, Blankenstein T. CD4+ T cell—mediated tumor rejection involves inhibition of angiogenesis that is dependent on IFN gamma receptor expression by nonhematopoietic cells. Immunity. 2000;12:677-686.
43. Fathallah-Shaykh HM, Zhao LJ, Kafrouni AI, Smith GM, Forman J. Gene transfer of IFN-gamma into established brain tumors represses growth by antiangiogenesis. J Immunol. 2000; 164:217-222.